

## Scaling of the $F_2$ structure function in nuclei and quark distributions at $x > 1$

N. Fomin,<sup>1,2</sup> J. Arrington,<sup>3</sup> D. B. Day,<sup>1</sup> D. Gaskell,<sup>4</sup> A. Daniel,<sup>5</sup> J. Seely,<sup>6</sup> R. Asaturyan,<sup>7,\*</sup> F. Benmokhtar,<sup>8</sup> W. Boeglin,<sup>9</sup> B. Boillat,<sup>10</sup> P. Bosted,<sup>4</sup> A. Bruell,<sup>4</sup> M. H. S. Bukhari,<sup>5</sup> M. E. Christy,<sup>11</sup> E. Chudakov,<sup>4</sup> B. Clasie,<sup>6</sup> S. H. Connell,<sup>12</sup> M. M. Dalton,<sup>1</sup> D. Dutta,<sup>13,14</sup> R. Ent,<sup>4</sup> L. El Fassi,<sup>3</sup> H. Fenker,<sup>4</sup> B. W. Filippone,<sup>15</sup> K. Garrow,<sup>16</sup> C. Hill,<sup>1</sup> R. J. Holt,<sup>3</sup> T. Horn,<sup>8,4</sup> M. K. Jones,<sup>4</sup> J. Jourdan,<sup>10</sup> N. Kalantarians,<sup>5</sup> C. E. Keppel,<sup>4,11</sup> D. Kiselev,<sup>10</sup> M. Kotulla,<sup>10</sup> R. Lindgren,<sup>1</sup> A. F. Lung,<sup>4</sup> S. Malace,<sup>11</sup> P. Markowitz,<sup>9</sup> P. McKee,<sup>1</sup> D. G. Meekins,<sup>4</sup> T. Miyoshi,<sup>17</sup> H. Mkrtchyan,<sup>7</sup> T. Navasardyan,<sup>7</sup> G. Niculescu,<sup>18</sup> Y. Okayasu,<sup>17</sup> A. K. Opper,<sup>19</sup> C. Perdrisat,<sup>20</sup> D. H. Potterveld,<sup>3</sup> V. Punjabi,<sup>21</sup> X. Qian,<sup>14</sup> P. E. Reimer,<sup>3</sup> J. Roche,<sup>19,4</sup> V.M. Rodriguez,<sup>5</sup> O. Rondon,<sup>1</sup> E. Schulte,<sup>3</sup> E. Segbefia,<sup>11</sup> K. Slifer,<sup>1</sup> G. R. Smith,<sup>4</sup> P. Solvignon,<sup>3</sup> V. Tadevosyan,<sup>7</sup> S. Tajima,<sup>1</sup> L. Tang,<sup>4,11</sup> G. Testa,<sup>10</sup> R. Trojer,<sup>10</sup> V. Tvaskis,<sup>11</sup> W. F. Vulcan,<sup>4</sup> C. Wasko,<sup>1</sup> F. R. Wesselmann,<sup>21</sup> S. A. Wood,<sup>4</sup> J. Wright,<sup>1</sup> and X. Zheng<sup>1,3</sup>

<sup>1</sup>University of Virginia, Charlottesville, VA, USA

<sup>2</sup>University of Tennessee, Knoxville, TN, USA

<sup>3</sup>Physics Division, Argonne National Laboratory, Argonne, IL, USA

<sup>4</sup>Thomas Jefferson National Laboratory, Newport News, VA, USA

<sup>5</sup>University of Houston, Houston, TX, USA

<sup>6</sup>Massachusetts Institute of Technology, Cambridge, MA, USA

<sup>7</sup>Yerevan Physics Institute, Armenia

<sup>8</sup>University of Maryland, College Park, MD, USA

<sup>9</sup>Florida International University, Miami, FL, USA

<sup>10</sup>Basel University, Basel, Switzerland

<sup>11</sup>Hampton University, Hampton, VA, USA

<sup>12</sup>University of Johannesburg, South Africa

<sup>13</sup>Mississippi State University, Jackson, MS, USA

<sup>14</sup>Duke University, Durham, NC, USA

<sup>15</sup>Kellogg Radiation Laboratory, California Institute of Technology, Pasadena, CA, USA

<sup>16</sup>TRIUMF, Vancouver, British Columbia, Canada

<sup>17</sup>Tohoku University, Sendai, Japan

<sup>18</sup>James Madison University, Harrisonburg, VA, USA

<sup>19</sup>Ohio University, Athens, OH, USA

<sup>20</sup>College of William and Mary, Williamsburg, VA, USA

<sup>21</sup>Norfolk State University, Norfolk, VA, USA

(Dated: May 11, 2018)

We present new data on electron scattering from a range of nuclei taken in Hall C at Jefferson Lab. For heavy nuclei, we observe a rapid falloff in the cross section for  $x > 1$ , which is sensitive to short range contributions to the nuclear wave-function, and in deep inelastic scattering corresponds to probing extremely high momentum quarks. This result agrees with higher energy muon scattering measurements, but is in sharp contrast to neutrino scattering measurements which suggested a dramatic enhancement in the distribution of the ‘super-fast’ quarks probed at  $x > 1$ . The falloff at  $x > 1$  is noticeably stronger in  $^2\text{H}$  and  $^3\text{He}$ , but nearly identical for all heavier nuclei.

PACS numbers: 13.60.Hb, 24.85.+p, 25.30.Fj

The quark structure of nuclei is extremely complex, and a detailed understanding of nuclei at the quark level requires the careful incorporation of nucleonic degrees of freedom and interactions as well as the dynamics of quarks and gluons. In inclusive electron scattering from nuclei, the cross section is characterized by the structure functions  $F_1(\nu, Q^2)$  and  $F_2(\nu, Q^2)$ , where  $\nu$  is the energy transfer and  $-Q^2$  is the square of the four-momentum transfer. At high  $Q^2$ , the reaction is dominated by elastic scattering from quasi-free quarks, and one can probe the momentum distribution of the quarks. In the Bjorken limit ( $\nu, Q^2 \rightarrow \infty$ ), the quark mass and transverse momenta are negligible compared to the energy and momentum of the probe, and the scattering is sensitive only to the the quark longitudinal momen-

tum, where  $x = Q^2/(2M\nu)$  is the fraction of the hadrons longitudinal momentum carried by the quark in the infinite momentum frame. In this deep inelastic scattering (DIS) limit, the structure functions exhibit *scaling*, i.e.  $F_2(\nu, Q^2) \rightarrow F_2(x)$ , becoming independent of  $Q^2$  at fixed  $x$ , with  $F_2(x)$  proportional to a charge-weighted sum of the quark momentum distributions in the target.

As one moves away from the Bjorken limit, there are deviations from perfect scaling. At finite- $Q^2$ , kinematical corrections yield a  $Q^2$  dependence that can be large for low  $Q^2$  or large  $x$ . While these scaling violations have historically been called ‘‘target mass’’ corrections [1], they are in fact independent of the mass of the target for a quark of a given longitudinal momentum. At lower  $Q^2$ , there are also significant contributions from higher twist

effects, e.g. structure due to quark–quark and quark–gluon correlations which appear most clearly as strong resonance structure. These scaling violating terms make extraction of the quark distributions most straightforward at high energies. QCD evolution yields an approximately logarithmic  $Q^2$  dependence at all  $Q^2$  values, but this is a true scale dependence of the parton distributions.

The early expectation was that the nuclear quark momentum distribution would be a convolution of the distribution of nucleons in a nucleus with the the distribution of quarks in the nucleons. Contrary to these expectations, measurements of inclusive scattering from nuclei showed a 10–20% suppression of high momentum quarks ( $0.3 < x < 0.8$ ) in heavy nuclei [2], demonstrating that the quark distributions in nuclei are not simply a sum of the proton and neutron’s quark distributions.

The quark distribution at  $x > 1$  is extremely small in the convolution model, as the nucleon quark distributions fall rapidly as  $x \rightarrow 1$  and there are very few fast nucleons available to boost the quarks to  $x > 1$ . The bulk of these ‘super-fast’ quarks come from nucleons above the Fermi momentum, which are generated by the strongly repulsive core of the N–N interaction; they reflect the short-range correlations (SRCs) in the ground state nuclear wave-function [3, 4]. Exotic configurations, such as 6-quark bags, may provide an even more efficient mechanism for generating very high momentum quarks, as the quarks from two nucleons can more freely share momentum [2, 4]. It is clear that a holistic explanation of DIS from nuclei must describe the behavior of the structure functions in the full kinematic range, and measurements at  $x > 1$  are necessary to illuminate the presence of short range structure in nuclei.

There are only two high energy measurements thus far for  $x \gtrsim 1$ , and they yield dramatically different results. Muon scattering data from the BCDMS collaboration [5] for  $Q^2$  from 52–200 GeV<sup>2</sup> show a rapid falloff in  $F_2(x)$ . They find  $F_2(x) \propto \exp(-s \cdot x)$  with  $s = 16.5 \pm 0.6$  for  $0.75 < x < 1.05$ , which suggests the need for relatively modest contributions from short-range correlations. Neutrino scattering measurements from the CCFR collaboration [6] at  $Q^2 = 125$  GeV<sup>2</sup> yield  $s = 8.3 \pm 0.7$  for  $0.75 < x < 1.2$ , which has been interpreted as an indication of exceptionally large strength from short-range correlations or the need for other, more exotic, contributions. However, both measurements have important limitations: CCFR had to make significant corrections due to the poor resolution on their reconstructed  $x$  value, while BCDMS was only able to extract  $F_2$  up to  $x = 1.05$ . It is unclear if this is sufficient to make meaningful comparisons to model predictions of short range structure in nuclei, as this is not expected to dominate until  $x \gtrsim 1.2$  [7, 8]. More extensive measurements have been made at lower energies, but they have been limited to  $x \approx 1$  [9, 10] or  $Q^2 < 5$  GeV<sup>2</sup> [11–13].

We present the results of JLab E02-019, which made

new measurements of inclusive scattering from nuclei, covering an expanded range in  $x$  and  $Q^2$ . Data were taken for few-body and heavy nuclei, covering both the region of the EMC effect [14] and  $x > 1$ . The measurement was performed in Hall C at the Thomas Jefferson National Accelerator Facility in 2004. A continuous wave electron beam of 5.766 GeV and current of  $\approx 80 \mu\text{A}$  was supplied. Electrons scattered from the target were detected using the High Momentum Spectrometer (HMS) at  $\theta = 18^\circ, 22^\circ, 26^\circ, 32^\circ, 40^\circ$ , and  $50^\circ$ , corresponding to  $2 \lesssim Q^2 \lesssim 9$  GeV<sup>2</sup>. Data were taken on cryogenic <sup>2</sup>H, <sup>3</sup>He, <sup>4</sup>He targets, solid Be, C, Cu, and Au targets, as well as Al targets used to measure and correct for the contribution from the walls of the cryogenic target cells.

Electrons were selected using the HMS gas Čerenkov and electromagnetic calorimeter detectors with efficiencies of  $>98\%$  and  $>99.7\%$ , respectively, and negligible pion contamination. Data were also taken with the HMS in positive polarity to determine the contribution from charge-symmetric processes. The systematic error associated with positron subtraction was negligible except at the largest  $Q^2$  values, where it is under 2%. The uncertainty due to the spectrometer acceptance is 1.4%.

The largest sources of systematic uncertainty at high  $x$  come from the beam energy (0.05%), HMS central momentum (0.05%) and angle (0.5mr) settings. The impact of these on the cross section is typically small (1–2% for  $x < 1$ ) for all but the largest  $x$  values, where the uncertainty can reach 4–6%. The systematic uncertainty that arises from subtraction of the aluminum end-caps (cryogenic targets only) also grows with increasing  $x$  values, as does the relative contribution of the aluminum end-caps to the measured cross section, giving a range in error of 0.3–2.4%. The cross sections also had to be corrected for bin-centering, radiative, and Coulomb effects. The systematic errors associated with those corrections are 0.5%, 1.4%, and  $<2\%$ , respectively. Details on the analysis and uncertainties, as well as the various corrections applied can be found in Ref. [15]. The total systematic uncertainty on the extracted cross sections is below 4% for  $x < 1$ , and up to 6% in the  $1 < x \lesssim 2$  range.

The structure function per nucleon,  $F_2(\nu, Q^2)$ , is extracted from the measured cross section as follows:

$$F_2 = \frac{d^2\sigma}{d\Omega dE} \cdot \frac{\nu}{\sigma_{mott}[1 + 2 \tan^2(\theta/2) \frac{1+\nu^2/Q^2}{1+R}]}, \quad (1)$$

with  $R = \sigma_L/\sigma_T = (0.32 \text{ GeV}^2)/Q^2$  [9] and  $\delta R/R = 50\%$ , yielding an additional uncertainty of  $\lesssim 1\%$  in  $F_2$ .

Scaling of the proton structure functions has been observed over a large kinematic range in high energy inclusive scattering. Based on these measurements, the DIS region is often taken to be  $W^2 > 4$  GeV<sup>2</sup>,  $Q^2 > 1$  GeV<sup>2</sup>, where  $W^2 = M_p^2 + 2M_p\nu - Q^2$  is the square of the invariant mass of the undetected hadronic system and  $M_p$  is the proton mass. It has been shown that scaling

violations are reduced when one examines  $F_2$  at fixed  $\xi = 2x/(1+r)$  [16], where  $r = \sqrt{1+Q^2/\nu^2}$ .  $\xi$  is equivalent to  $x$  in the Bjorken limit, but when examining scaling at fixed  $\xi$ , rather than fixed  $x$ , the observed scaling behavior extends to lower  $W^2$  [12, 13], corresponding to larger  $\xi$  values. This improved scaling can be seen clearly in Fig. 1, where the upper sets of curves show  $F_2$  for carbon plotted against  $x$  (red squares) and  $\xi$  (green circles) over a range of  $Q^2$  values. The extended  $\xi$ -scaling of the nuclear structure function, seen to begin above 3–4 GeV<sup>2</sup>, may allow access to quark distributions for  $\xi \gtrsim 1$  [17, 18].

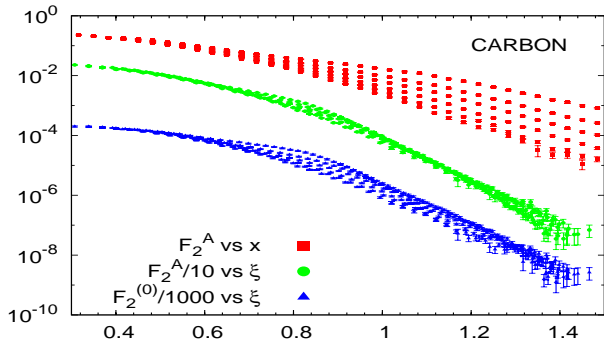


FIG. 1: (Color online)  $F_2$  for the E02-019 carbon data ( $2 \lesssim Q^2 \lesssim 9$  GeV<sup>2</sup>) as a function of  $x$  (top) and  $\xi$  (middle), and  $F_2^{(0)}$  vs  $\xi$  (bottom). In each case, the higher points correspond to the smaller scattering angles (lowest  $Q^2$  values).

We compare our data to higher  $Q^2$  measurements, using a partonic framework to look for deviations from the scaling picture. Rather than simply examining  $F_2$  as a function of  $\xi$ , as was done previously, we account for the kinematical scaling violations using the prescription of Ref. [1] (Eq.(23)) and study the scaling of  $F_2^{(0)}(\xi, Q^2)$ :

$$\frac{x^2}{\xi^2 r^3} F_2^{(0)}(\xi, Q^2) = F_2(x, Q^2) - \frac{6M^2 x^3}{Q^2 r^4} h_2(\xi, Q^2) - \frac{12M^4 x^4}{Q^4 r^5} g_2(\xi, Q^2), \quad (2)$$

where  $h_2(\xi, Q^2) = \int_{\xi}^A u^{-2} F_2^{(0)}(u, Q^2) du$  and  $g_2(\xi, Q^2) = \int_{\xi}^A v^{-2} (v - \xi) F_2^{(0)}(v, Q^2) dv$ . One could incorporate these effects into a partonic model for  $F_2$ , rather than extracting an “idealized” scaling function, but this approach minimizes the  $Q^2$  dependence in the scaling function, making it easier to directly compare different data sets.

To calculate  $h_2$  and  $g_2$ , we use a factorized model for  $F_2^{(0)}(\xi, Q^2)$ , with a common  $Q^2$  dependence for all targets and a simple fit to  $F_2^{(0)}(\xi, Q_0^2)$  for each nucleus. In the partonic picture, the  $Q^2$  dependence should come only from QCD evolution. Because we cannot determine QCD evolution without knowing the partonic structure, we fit the  $Q^2$  dependence of the world’s data (shown in Fig. 2), excluding our lower  $Q^2$  points, at several  $\xi$  values to a functional form chosen to be consistent with evolution. This is used to scale our new data to  $Q_0^2 = 7$  GeV<sup>2</sup>,

and we obtain a fit for  $F_2^{(0)}(\xi, Q_0^2)$  from a subset of these data, chosen to minimize contributions from quasielastic scattering. This simple fit provides a reasonable description of the global data set (see Fig. 2), with deviations at low  $Q^2$ , in particular near the quasielastic peak ( $\xi \approx 0.85$ ) and for the largest values of  $\xi$ . The  $h_2$  and  $g_2$  terms yield corrections of up to 15% at the lower  $Q^2$  values, but  $\lesssim 5\%$  for  $Q^2 > 5$  GeV<sup>2</sup>. We estimate the model dependence in the extraction of  $F_2^{(0)}$  to be  $\lesssim 2\%$ .

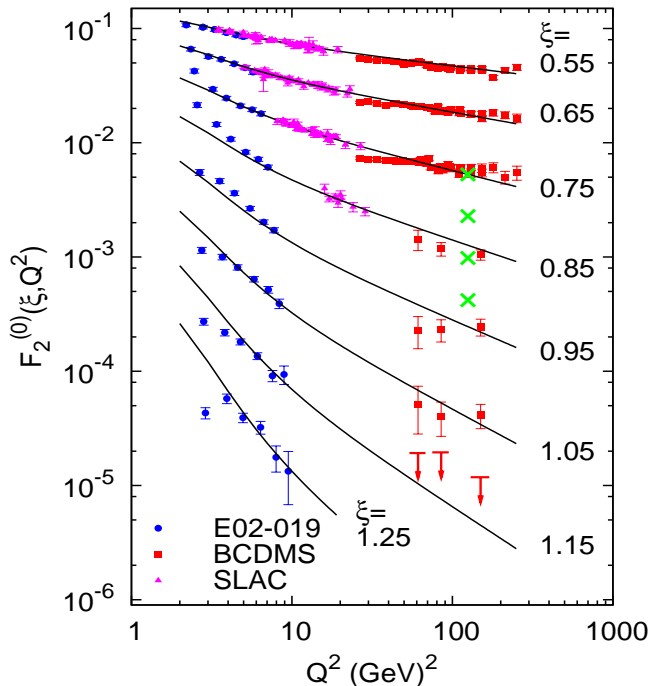


FIG. 2: (Color online)  $F_2^{(0)}$  vs  $Q^2$  for fixed  $\xi$  value. For this work and BCDMS, the carbon data are shown, while the SLAC points are carbon pseudo-data taken from measurements on deuterium. The solid curves are the global fit, the short horizontal red lines show the BCDMS  $\xi=1.15$  upper limit, and the green crosses show the falloff between  $\xi=0.75$  and  $\xi=1.05$  based on the CCFR data (see text for details).

Figure 1 shows  $F_2^{(0)}$  vs  $\xi$  (blue triangles), which has somewhat *greater*  $Q^2$  dependence at large  $\xi$  than the uncorrected structure function  $F_2$  (green circles). The main difference between  $\xi$ -scaling and our scaling analysis is the factor  $x^2/(\xi^2 r^3)$  in front of the leading term in Eq. 2, as the  $h_2$  and  $g_2$  terms are relatively small. Neglecting this pre-factor introduces an additional  $Q^2$  dependence that approximately cancels that of the QCD evolution, resulting in an artificially small  $Q^2$  dependence in the naive  $\xi$ -scaling analysis.

Figure 2 shows the carbon results for  $F_2^{(0)}(\xi, Q^2)$ , scaled to fixed values of  $\xi$  using our global fit. The SLAC points are deuterium data [19], multiplied by the SLAC E139 [20] fit to the carbon-to-deuteron structure function ratio, yielding carbon pseudo-data to provide a continu-

ous  $Q^2$  range for lower  $\xi$  values. For all data sets,  $F_2^{(0)}$  is extracted from the measured structure functions using the global fit to calculate  $g_2$  and  $h_2$ . For  $\xi \leq 0.75$ , where the high  $Q^2$  data determine the evolution, our data are in excellent agreement with this  $Q^2$  dependence down to  $Q^2 = 3 \text{ GeV}^2$ . The observed  $Q^2$  dependence grows slowly with  $\xi$  over this region, and with a continued increase at higher  $\xi$  values, our highest  $Q^2$  measurements are consistent with SLAC and BCDMS. For large  $\xi$  values at low  $Q^2$ , our data deviate from this  $Q^2$  dependence due to higher twist contributions, especially in the vicinity of the quasielastic peak ( $\xi \approx 0.85$ )

The CCFR measurement did not explicitly extract values of  $F_2$ , but obtained a fit to the falloff at large  $\xi$ . We illustrate this falloff by normalizing to our global fit at  $\xi = 0.75$  and applying the CCFR  $\xi$  dependence to extract  $F_2^{(0)}$  at  $\xi = 0.75, 0.85, 0.95$ , and  $1.05$ , shown as green crosses. This behavior is clearly inconsistent with the overall behavior of the structure function extracted from electron and muon scattering. The BCDMS data exhibit somewhat unusual behavior at large  $\xi$ . Above  $\xi = 0.65$ , the BCDMS data show little or no  $Q^2$  dependence, even though one expects noticeable QCD evolution.

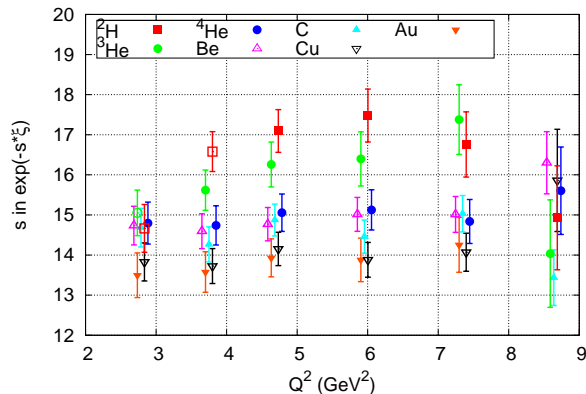


FIG. 3: (Color online) The slope  $s$  in  $\exp(-s \cdot \xi)$  as a function of  $Q^2$ . The targets are offset in  $Q^2$  for visibility. Open symbols for  ${}^2\text{H}$  and  ${}^3\text{He}$  at low  $Q^2$  are cases where the kinematic limit for the nucleus ( $x \approx A$ ) corresponds to  $\xi \lesssim 1.25$ .

To quantitatively examine the falloff of our structure function at large  $\xi$ , we perform a fit similar to BCDMS and CCFR. We take the data from a fixed scattering angle, use the global fit to interpolate to a fixed  $Q^2$  value (corresponding to  $\xi = 1.1$ ), and fit  $F_2^{(0)}(\xi, Q^2)$  to  $\exp(-s \cdot \xi)$  for  $1 < \xi < 1.25$ . The lower  $\xi$  limit is chosen to avoid regions where the quasielastic peak leads to noticeable deviations from scaling at low  $Q^2$ , and the upper  $\xi$  limit is chosen so that there are data covering the full  $\xi$  range for all targets and  $Q^2$  values. We take the slope extracted from the  $40^\circ$  data ( $Q^2 = 7.35 \text{ GeV}^2$ ) as the main result, as this is the largest  $Q^2$  value with high statistics over the full  $\xi$  range. Data at smaller angles are used to examine

the  $Q^2$  dependence of the result.

TABLE I: Extracted values of the slopes for all nuclei. The uncertainties includes statistics and systematics; the latter are typically  $\sim 0.4$  and dominate the uncertainty.

A	$Q^2 = 2.79$	3.75	4.68	5.95	7.35
2	$14.7 \pm 0.6$	$16.6 \pm 0.5$	$17.1 \pm 0.5$	$17.5 \pm 0.7$	$16.8 \pm 0.8$
3	$15.1 \pm 0.6$	$15.6 \pm 0.5$	$16.6 \pm 0.6$	$16.4 \pm 0.7$	$17.4 \pm 0.9$
4	$14.8 \pm 0.5$	$14.7 \pm 0.5$	$15.1 \pm 0.5$	$15.1 \pm 0.5$	$14.8 \pm 0.6$
9	$14.7 \pm 0.5$	$14.6 \pm 0.4$	$14.8 \pm 0.4$	$15.0 \pm 0.4$	$15.0 \pm 0.5$
12	$14.7 \pm 0.5$	$14.3 \pm 0.4$	$14.9 \pm 0.4$	$14.5 \pm 0.4$	$15.0 \pm 0.5$
64	$13.8 \pm 0.5$	$13.7 \pm 0.4$	$14.2 \pm 0.4$	$13.9 \pm 0.4$	$14.1 \pm 0.5$
197	$13.5 \pm 0.6$	$13.6 \pm 0.5$	$13.9 \pm 0.5$	$13.9 \pm 0.5$	$14.3 \pm 0.7$

The extracted slopes are shown in Table I and Fig. 3. Above  $4 \text{ GeV}^2$ , there is no systematic  $Q^2$  dependence, and at lower  $Q^2$ , only the  ${}^2\text{H}$  and  ${}^3\text{He}$  results change significantly. We observe nearly identical behavior in the high- $\xi$  falloff for all nuclei except  ${}^2\text{H}$  and  ${}^3\text{He}$ , which have a larger slope and thus a steeper falloff with  $\xi$ .

We obtain  $s = 15.0 \pm 0.5$  for carbon,  $s = 14.1 \pm 0.5$  for copper (our closest nucleus to the CCFR iron target), showing that the large difference between BCDMS and CCFR is not related to the difference in target nuclei. Note that BCDMS and CCFR extract slopes from  $F_2(x)$  instead of  $F_2^{(0)}(\xi)$ , although the difference would increase their slopes by less than 0.5 (0.1) for the BCDMS (CCFR). Further complicating direct comparison is the fact that none of these experiments cover the same  $\xi$  range. For our new data, variations in the  $\xi$  limits of 0.05–0.1 can change the extracted slope by 0.5–1.0.

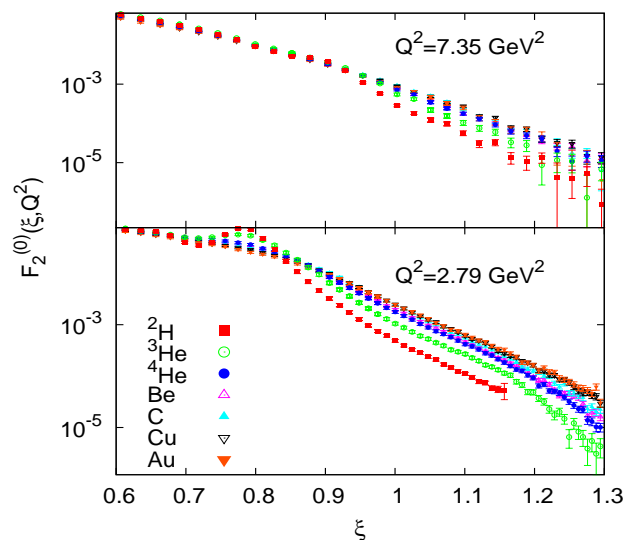


FIG. 4: (Color online) The extracted scaling structure function per nucleon for all nuclei at  $Q^2 = 2.79$  and  $7.35 \text{ GeV}^2$ . The deuteron data are kinematically limited to  $x < 2$ , corresponding to  $\xi \lesssim 1.15$  for the low  $Q^2$  setting.

We have focused on heavier nuclei for comparison to BCDMS and CCFR, but have also obtained a significantly expanded body of data for light nuclei, shown in Fig. 4. At low  $Q^2$ , the light nuclei show a clear quasielastic peak, while at higher  $Q^2$  the peak is almost entirely washed out. For heavier nuclei, the extracted scaling function per nucleon is nearly identical at all  $\xi$  values. However, for  $^2\text{H}$  and  $^3\text{He}$ , there is a significant reduction in strength for  $\xi \gtrsim 1$ , which is observed at all  $Q^2$  values.

In summary, we have made extensive measurements of the large  $\xi$  structure functions for  $Q^2$  from 2–9  $\text{GeV}^2$ . We have extracted the scaling structure function,  $F_2^{(0)}(\xi, Q^2)$ , and shown that it is consistent with a nearly logarithmic  $Q^2$  dependence over a significant range of  $\xi$  and  $Q^2$ . These new data do not show a need for extremely large contributions from short-range correlations or other, more exotic, short range structures, as suggested by the CCFR result. The large  $\xi$  behavior of our data is consistent with the BCDMS results, but our results extend to significantly higher  $\xi$  values, where one expects to be most sensitive to short range structure [4, 8]. The new data, covering a range of nuclei at large  $\xi$ , can be used to directly constrain calculations of the effect of short-range correlations or multi-quark configurations in our kinematic regime for a wide range of nuclei. A future 12 GeV JLab measurement [21] will double the  $Q^2$  range for these  $\xi$  values, moving to a region where we can directly extract the parton distributions of the super-fast quarks in nuclei.

We thank the JLab technical staff and accelerator division for their contributions. This work supported in part by the NSF and DOE, including grant NSF-0244899 and DOE contracts DE-FG02-96ER40950, DE-AC02-

06CH11357 and DE-AC05-06OR23177 under which JSA, LLC operates JLab, and the South African NRF.

---

\* Deceased

- [1] I. Schienbein et al., J. Phys. **G35**, 053101 (2008).
- [2] D. F. Geesaman, K. Saito, and A. W. Thomas, Ann. Rev. Nucl. Sci. **45**, 337 (1995).
- [3] L. L. Frankfurt, M. I. Strikman, D. B. Day, and M. Sargsian, Phys. Rev. C **48**, 2451 (1993).
- [4] M. M. Sargsian et al., J. Phys. **G29**, R1 (2003).
- [5] A. Benvenuti et al. (BCDMS), Z. Phys. **C63**, 29 (1994).
- [6] M. Vakili et al. (CCFR), Phys. Rev. D **61**, 052003 (2000).
- [7] J. Rozynek and M. C. Birse, Phys. Rev. **C38**, 2201 (1988).
- [8] L. L. Frankfurt and M. I. Strikman, Phys. Rept. **160**, 235 (1988).
- [9] P. Bosted et al., Phys. Rev. C **46**, 2505 (1992).
- [10] J. Arrington et al., Phys. Rev. C **53**, 2248 (1996).
- [11] D. B. Day et al., Phys. Rev. Lett. **43**, 1143 (1979).
- [12] B. W. Filippone et al., Phys. Rev. C **45**, 1582 (1992).
- [13] J. Arrington et al., Phys. Rev. C **64**, 014602 (2001).
- [14] J. Seely et al., Phys. Rev. Lett. **103**, 202301 (2009).
- [15] N. Fomin, Ph.D. thesis, University of Virginia (2007), arXiv:0812.2144.
- [16] O. Nachtmann, Nucl. Phys. **B63**, 237 (1973).
- [17] J. Arrington, R. Ent, C. E. Keppel, J. Mammei, and I. Niculescu, Phys. Rev. C **73**, 035205 (2006).
- [18] W. Melnitchouk, R. Ent, and C. Keppel, Phys. Rept. **406**, 127 (2005).
- [19] L. W. Whitlow, E. M. Riordan, S. Dasu, S. Rock, and A. Bodek, Phys. Lett. **B282**, 475 (1992).
- [20] J. Gomez et al., Phys. Rev. D **49**, 4348 (1994).
- [21] J. Arrington, D. B. Day, et al. (2006), JLab Proposal E12-06-105.